

Modern trends in selecting and designing Kaplan turbines

PART ONE

By F. de Siervo and F. de Leva*

Results of an extensive investigation carried out on more than 130 Kaplan turbines manufactured all over the world are presented in the form of statistical diagrams providing engineers with the latest information for preliminary design of hydro powerplants.

THIS PAPER presents the results of a study on the present state of the art in the design of hydraulic machines, of which the first part concerning Francis type turbines was published in August 1976 issue of this magazine¹.

For simplicity, considerations that are common to both Francis and Kaplan turbines are not repeated in this paper; the authors suggest therefore that reference to the previous article will give a better understanding of the present subject.

Whenever it has been deemed advisable, comparisons have been made between Francis and Kaplan design criteria and dimensions, particularly for those machine components that are similar from the hydraulic point of view, such as the steel spiral case and the draft tube.

The data collected show that the trend towards greater capacities is less pronounced for Kaplan than for Francis machines. In the field of high head units this appears to be the consequence of the competitiveness of Francis turbines which are less expensive, while for low heads the upper capacity limit is set by the actual dimensions of the machines. The research covers, with some exceptions, the period between 1960 and 1976.

Table I gives the main features of the installations investigated as taken from the references, while the diagrams are based on the project data and dimensions collected by an extensive inquiry carried out through both questionnaires sent to the most important manufacturers and from visits to several made by one of the authors.

The curves were drawn by a simple regression procedure, using the same digital computer program adopted in the previous study on Francis turbines.

*E.L.C. - Electroconsult, Via Chiebrara 8, 20151 Milan, Italy.

Table I—Kaplan turbines at major hydro schemes

Powerplant	Manufacturer	Year	Head (ft)	Capacity (MW)	Rotation frequency (rev/min)
Agulhas	Hitachi	1963	14.44	31	88
Akkata (1)	Nohab	1973	41.8	109	115.4
Americah Falls	Voest-Alpine	1978	31.6	31.3	130
Arbon	Vevey	1963	25.4	38.1	136
Arias	Charmilles		15.2	5.43	136.5
Azchach	Voith	1969	15.3	69.85	88.3
Azutan	Eschner Wyss	1966	24.6	68	115.4
Beaumont Durance (2)	Neyrpic	1965	18.6	19.85	123
Boden	KMW	1964	12.2	39.6	93.8
Boomerie	Allis Chalmers	1976	21.3	78.3	69.2
Brokponde	Eschner Wyss	1972	44.2	39	240
Byaforsen	KMW	1973	9.3	17	93.8
Carbonne	Vevey	1966	11.5	17.15	176
Carillon	Dominion	1962	17.98	44.1	97.3
Cedillo	Eschner Wyss	1971	43	110	93.8
Carnedilla	Nohab	1969	35.6	30.65	250
Chili Bar	Allis Chalmers	1962	17.3	7.15	200
117025 (China)	KMW	1972	18	44	115
Chong Pyong	Hitachi	1967	24	40	150
Clarence Cannon	Allis Chalmers	1968	18	31.3	129
Chuncheon	Toshiba	1963	28.8	30	150
Coisac	Vevey	1968	20.85	28.8	150
Cordet Hull (3)	Voest Alpine	1965	14	42.8	65.5
Cowans Ford	Allis Chalmers	1965	28	88.9	106
Drop No. 3	Allis Chalmers	1964	7.3	3.3	112.5
Dalles Dam (3)	Voest Alpine	1967	27	91.2	85.7
Dardanelle Lock (4)	Dominion	1964	14.6	38	75
Dneprodzhezhinsk	KHTBP	1962	12.5	48.2	51.7
Edea III	Vevey	1968	7.3	29.2	167
Feistritz	Charmilles		23.8	41.44	136.4
Foelach	Voith	1972	20.8	39	125
Follum	Voith	1975	27.5	29	187.5
Fratel (5)	Neyrpic	1969	22	45.6	150
Futunata	Mitsubishi	1960	35	16	333
Garmten	Eschner Wyss	1964	14.2	16.2	115.4
Gocho	Mitsubishi	1976	27.1	7.04	333.3
Gresifoss (6)	Kvaerner Brug	1965	30	21.32	214
Guajoyo	Toshiba	1963	54	19.75	300
Hallforsen	Nohab	1964	8.6	15.7	94
Harpefoss	Nohab	1964	32.45	46.05	150
Hirakud I	Hitachi	1961	36.3	38.8	150
Honbetau	Toshiba	1962	33	26	187
Ice Harbor	Allis Chalmers	1971	27.1	127.9	85.7
Isola Serafini	F. Toal	1957	7.50	12.5	53.6
Isola Serafini	Riva Calzoni	1957	7.50	12.5	53.6
Iwaonai	Mitsubishi	1970	51.37	13.45	333
Jordap Iron Gate	LMW	1969	36.5	178	71.5
Jupia (16)		1969	23	107	78.3
Kabokura	Fuji	1958		> 13.9	300
Kalnji	Voest Alpine	1974	38	139.7	107.2
Kamigo	Fuji	1961	18.1	> 17	167
Komoso II	Fuji	1970	22.1	> 35	107
Kanayama	Hitachi	1966	72.5	> 17.5	300
Kang Krachan	Fuji	1971	48	> 17.5	250
Karnafuli	Allis Chalmers	1969	23.7	50.7	115
Kasabori	Hitachi	1963	65.1	7.95	500
Kindaruna (7)	KMW	1965	32	23.9	214
Khashm el Girba	Ansaldo	1961	40	3.43	500
Klaus	Voith	1972	40.5	14.5	333.3
Krangfors III	KMW	1970	29.5	26.8	187.5
Krokstrommen	KMW	1961	57	50.5	231
Lavey (8)	Charmilles		43	30.9	214.3
Ligga III	Nohab	1961	39	> 181.7	107.1
Little Goose (3)	Voest Alpine	1963	31	158	90
Little Goose	Allis Chalmers	1974	28.3	156.1	90
Mactaquac	Dominion	1966	33.5	102.9	112.5
Manoquee	Charmilles		35.85	48	150
Marckolsheim (2)	Neyrpic	1957	15.4	40.8	75
Markland	Allis Chalmers	1962	10.3	30.5	64.3
Mascarenhas	Allis Chalmers	1969	17.5	40.4	106
McGee Bend	Allis Chalmers	1960	21.3	30.3	120
McSwain Dam	Allis Chalmers	1964	16.4	8.8	180
Melkefoss	KMW	1975	19	22.9	93.75
Metter-Tusnad	LMW	1963	48.8	56.7	136.4
Midorikawa II	Mitsubishi	1970	36.49	6.38	400
Myashita	Toshiba	1926	39.41	39	167
Mozoto (9)	Dominion	1975	21.9	108.8	80
Namforsen III	KMW	1970	21	58.3	100 6.5
Ohyodogawa I	Fuji	1961	40.4	42.2	180
Otori	Hitachi	1962	51	100	125
Ottmarshaim	Charmilles		17.4	41.3	93.75
Palmar	Neyrpic	1977	27.15	113.4	88.2
Palokongha	LMW	1965	11.8	10.2	68.2
Passo Real (10)	Dominion	1973	40.9	72.5	138.5
Porto Colombia (11)	Villamette				
	Nohab	1973	19.3	85.2	85.7
Radi	KMW	1973	23	103.7	100
Regua	KMW	1968	25.3	65	107.1
Rhinau	Charmilles		12.5	41.25	75
Robert S. Kerr	Allis Chalmers	1964	12.3	33.8	75
Rosieres I-3	Voest Alpine	1968	48	30.8	136.4
Rosieres IV	Voest Alpine	1976	48	> 44	136.4
Rygeho (12)	Kvaerner-Brug	1974	36.2	55.15	166.7

(Table I continued)

Salignac (13)	Neyrpic	1972	28	43.6	150
Saravali	Toal	1968	13.2	29.1	78.95
Saravali	KHTBP	1965	15	59.3	50
Sarp	Nohab	1978	21	> 82.7	93.8
Sant Moritz	Vevey	1962	26	31.7	150
Salingus	Voith	1976	18.4	> 11.9	125
Shimonikappa	Fuji		40.4	> 17.6	273
Shio-nokanan	Toshiba	1970	20	31	125
Shizmai	Toshiba	1966	47	25.6	300
Sobradelo	Vevey	1968	34	31.2	187.5
Sonohara II	Eschner Wyss	1962	46.3	5.6	500
St. Martin	Voith	1964	74.5	11	610
Subari	Hitachi	1970	63.1	6.62	500
Sveg	KMW	1973	19	34.2	115.4
Tabaol	LMW	1971	49	103	125
Tawara	Toshiba	1967	46.1	22.9	257
Tchi Li Long (14)	Neyrpic	1972	22	75	71.5
Tedorigawa III	Fuji				
Termaiso	Allis Chalmers	1964	25.9	33	138.5
Tinof II (15)	Kvaerner Brug	1973	29.2	20.15	214
Toyama	Fuji				
Toyomi II	Fuji				
Trail Bridge	Allis Chalmers	1960	20.4	8.6	212
Traunfall	Voest Alpine	1972	16.8	9.56	187.5
Tres Marias	Voith	1965	50	73.53	163.6
Tuggen	Nohab	1962	26.6	50.24	125
Tungabadr	Hitachi	1962	28.6	12.1	214
Tungabadr	Voest Alpine	1961	20	9.56	214.3
Ulam	Fuji				
Upper Toloma	LMW	1963	60	58.7	187.5
Valeria	Nohab	1975	27.2	83.53	115.4
Vamma (1)	Nohab	1970	27	110	100
Vilouvi	KHTBP	1963	68	79.5	187.5
Vopnagrun	Charmilles		15	35.3	83.3
Volga XXIII No. 22	LMW	1961	27	132	68.2
Volta Grande (9)	Dominion	1974	26.2	101.5	85.7
Votkinsk	LMW	1961	23.5	107	62.5
Wallase	Voith	1965	9.6	41.9	65.2
Wanapur	Dominion	1963	24.3	88.2	85.7
Weisshaus	Voest Alpine	1966	31	7.65	300
Wiingi	Toshiba	1976	20.7	27.8	143

- 1 In collaboration with KMW.
- 2 In collaboration with Alstom and Charmilles.
- 3 According to BLH drawing.
- 4 In conjunction with Bingham-Willamette.
- 5 In collaboration with Sorefame and Creusot-Loire.
- 6 In collaboration with KMW.
- 7 In collaboration with Boving.
- 8 In collaboration.
- 9 In collaboration with General Electric S.A., Brazil.
- 10 Design and model test only; manufactured by Bingham-Willamette.
- 11 In collaboration with Bardella S.A.
- 12 In collaboration with Tampella.
- 13 In collaboration with Creusot-Loire and Jeumont-Schneider.
- 14 In collaboration with Creusot-Loire.
- 15 In collaboration with Voith.
- 16 KQYL joint venture Asgen-Eschner Wyss-Riva Calzoni.

The value of the correlation coefficients and standard deviations indicated in the test permit in each case, the evaluation of the degree of association between the two variables under study and of the scattering of the data in respect of the interpolating function.

General selection criteria

The same characteristics constant used for Francis is adopted for the Kaplan turbines.

$$n_s = n P_t^{0.8} H_n^{-1.25} \quad \dots (1)$$

and the relationship

$$n_s = n_s(H_n)$$

is sought between the specific speed and the design head.

The available data have been divided into three groups, depending on the year of design of the turbines. This gives the three regression curves indicated in Fig. 1, which are described as follows:

$$\begin{aligned} 1960-1964 \quad n_s &= 2.096 H_n^{-4.89} \\ 1965-1969 \quad n_s &= 2.195 H_n^{-4.89} \\ 1970-1976 \quad n_s &= 2.419 H_n^{-4.89} \quad \dots (2) \end{aligned}$$

The correlation coefficients and the standard deviations are respectively:

$$\begin{aligned} r &= -.92 & s &= 57.2 \\ r &= -.92 & s &= 55.3 \\ r &= -.89 & s &= 47.6 \end{aligned}$$

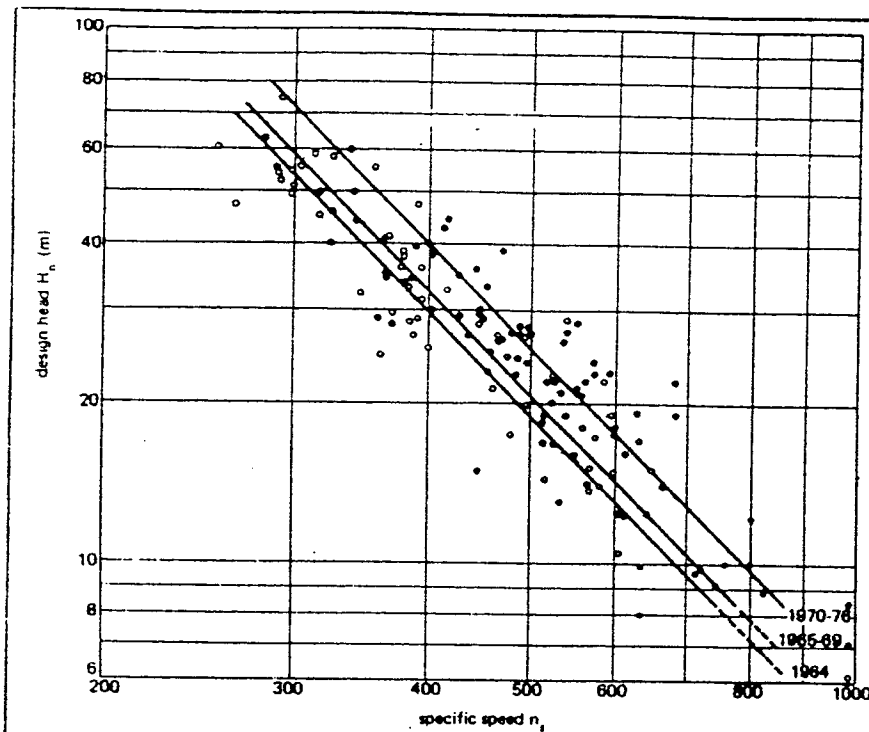


Fig. 1. Specific speed versus design head. Curves are drawn for three groups of machines depending on the year of design.

Notations*

- D_M = Runner outer diameter (m)
- g = Gravity acceleration (m/s^2)
- h_b = Barometric pressure (m)
- h_s = Static suction head referred to the wicket gate centreline (m)
- h_w = Water vapour pressure (m)
- H_n = Turbine net design head (m)
- k_u = Runner peripheral velocity coefficient
- k_{v1} = Ratio between water velocity v_1 and spouting velocity
- k_{v2} = Ratio between water velocity v_2 and spouting velocity
- n = Turbine speed of rotation (rev/min)
- n_f = Turbine runaway speed of rotation (rev/min)
- n_s = Turbine specific speed
- P_t = Turbine design capacity (kW)
- Q_v = Turbine rated flow (m^3/s)
- QY = Flow passing through a spiral case radial section rotated by the angle γ in respect of the spiral nose (m^3/s)
- r = Statistical curves correlation coefficient
- r_l = Distance of a point in the spiral case from the turbine axis (m)
- s = Statistical curves standard deviation
- v_1 = Water velocity at steel spiral cases inlet section (m/s)
- v_2 = Water velocity at concrete cases inlet section (m/s)
- v_3 = Water velocity at draft tube inlet section (m/s)
- v_u = Peripheral velocity of water in the spiral case
- σ = Cavitation coefficient (Thoma's coefficient)

*For notations relevant to the machine main dimensions refer to the relevant figures.

They show a high degree of grouping of the data in respect to the chosen interpolating functions.

As for the Francis turbines, the diagram shows that, over the period considered, there has been a trend to increase the value of n_s for a given head, that has become more evident in the last years. By comparing the n_s given in Fig. 1 with the n_s relevant to Francis turbines for the same period, one sees that in the overlapping area (n_s ranging from 250 to 350) the specific speed is clearly higher for Kaplan turbines while the slope of the curves is comparable. Proposition developed later in this article show that, notwithstanding the higher n_s value, Kaplan turbines are larger than Francis types for a given capacity.

As for Francis turbines, the curves of Fig. 1 show the specific speed n_s corresponding to an average statistic value of the most significant existing installations for assigned heads, and therefore they serve only to give an indicative value. Single installations may have n_s values

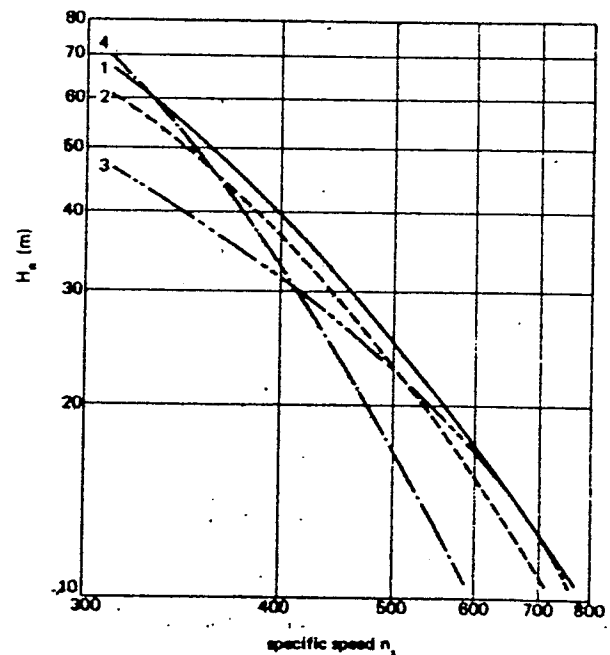


Fig. 2. Increase of specific speed (for a given head) as a function of the period of design. Curve no. 1 is derived from Fig. 1; curve no. 2 is taken from "Handbook of applied hydraulic" Sorensen, K. E. and C. V. Davis 1969; curve no. 3 is taken from "Turbines hydrauliques et leur regulation" by L. Vivier, 1966; and curve no. 4 is derived from US Bureau of Reclamation's "Selecting hydraulic reaction turbines", 1966.

that differ from those given by the equations, depending on particular operating or design criteria as was shown for Francis turbines. Therefore these equations should be used with some degree of precaution adapting the calculated values to the particular characteristics of the installation under consideration.

The curves shown on Fig. 2 confirm the general trend towards higher specific speeds for a given head.

Once the value of n_s is decided from Fig. 1, the best rotation frequency is determined by Eq. (1); the rated frequency of the turbine will coincide with one of the synchronous frequencies nearest to the ideal one; the higher or lower value will be chosen, depending on

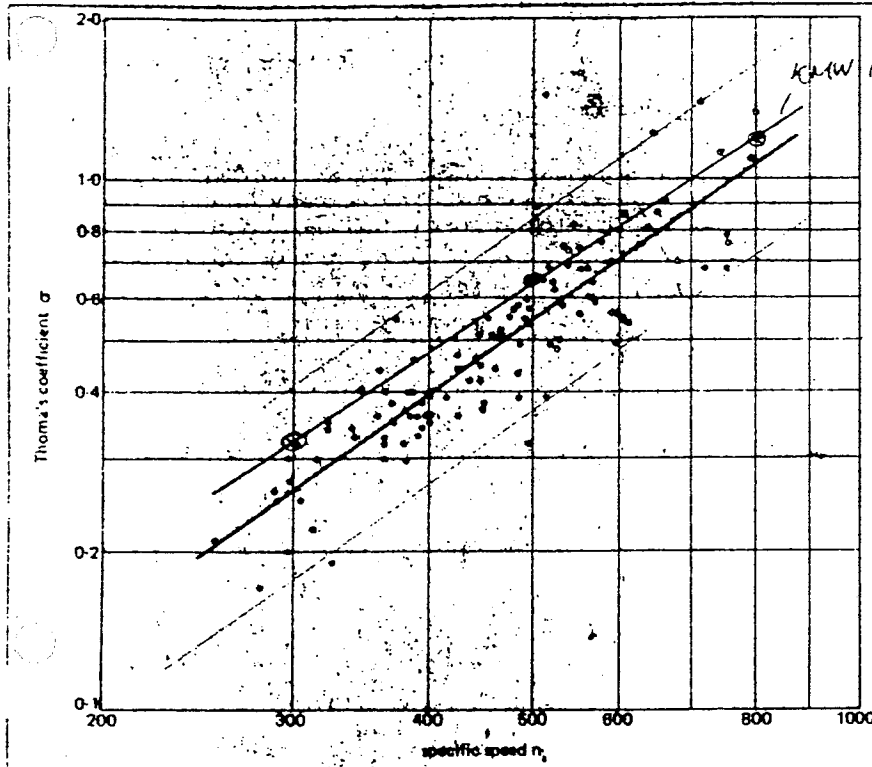


Fig. 3. Cavitation (Thoma's) coefficient versus specific speed.

technical and economic considerations similar to those indicated already for Francis turbines.

The chosen synchronous speed will then determine the actual n_s value to be used for entering the subsequent diagrams.

The cavitation coefficient is expressed by the formula:

$$\sigma = (h_b - h_w - h_s) / H_n$$

The σ values have been calculated for the design head H_n , taking $h_b - h_w = 9.8$ m for all the examined installations. This roughly corresponds to an average turbine installation level of 200 m and to a mean water temperature of 20°C.

In some cases the values indicated here do not represent the most severe operating conditions that correspond instead to the maximum head which, for Kaplan turbines, often occurs with the tailwater level at its minimum value.

The operating σ value and consequently the installation level of the machine can in such a case be correctly determined only by the performance diagram of the turbine.

The available data have led to the following relation between σ and n_s :

$$\sigma = 6.40 \cdot 10^{-5} n_s^{1.48}$$

with

$$r = 0.88 \quad s = 0.14$$

The corresponding curve is given in Fig. 3.

In Fig. 4 the calculated curve is compared with similar ones taken from the literature.

The reduction in the values of Thoma's coefficient for a given n_s , as it appears in Fig. 4, is a result of improvements in the hydraulic design of the machines, leading to lower values of the submergence and consequently to considerable cost saving of the civil works.

The suction head H_s , calculated on the basis of the average 1970-1976 on Fig. 1 and of the σ curve on Fig. 3, is shown in Fig. 5.

The average suction head ranges between -1 and -8 m in the range of n_s considered.

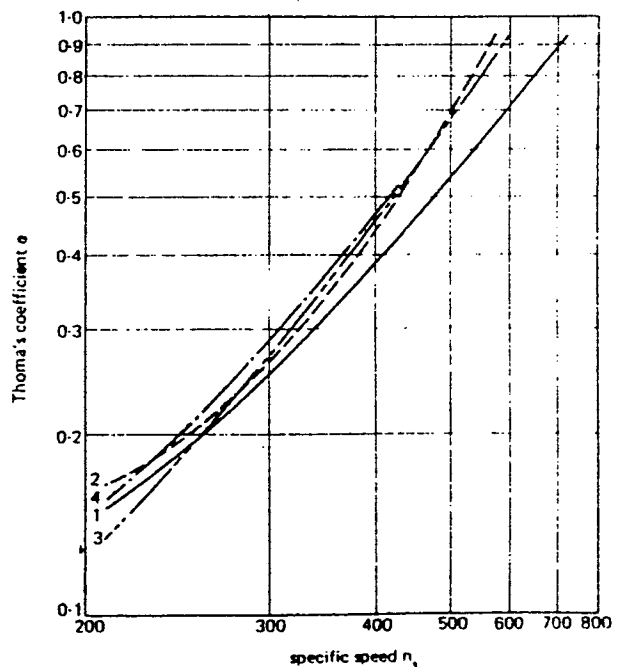


Fig. 4. Cavitation (Thoma's) coefficient decrease (for a given n_s) as a function of the period of design. The curve denoted by 1 is the one given in Fig. 3, while curves 2, 3 and 4 are derived from the same sources indicated in Fig. 2.

By comparing Fig. 3 with the corresponding figure for Francis turbines it can be seen that while both $\sigma - \sigma(n_s)$ curves show the same slope, the average σ values are for Kaplan turbines approximately 10 per cent higher than for Francis with the same n_s value.

The ratio between the runaway rotation frequency n_f (off-cam values) and the rated one is expressed as a function of n_s in Fig. 6.

As for Francis turbines the scattering shown by the diagram can be attributed to the width of the range of operating head of the machines.

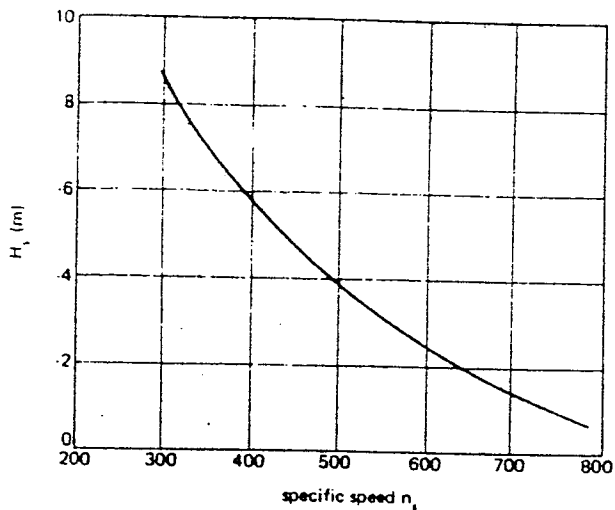


Fig. 5. Suction head versus specific speed.

The interpolating function is:

$$n_f/n = 2.44 + 2.04 \cdot 10^{-4} n_s$$

with

$$r=0.09 \quad s=0.28$$

The remarkable difference in behaviour between Kaplan and Francis turbines in runaway conditions is explained by the following two considerations:

- the positive slope of the Francis curve is given by the centrifugal effect characteristic of Francis runners, which decreases with increasing n_s , because of the change in shape of the runner. This effect does not occur in Kaplan turbines and explains the much flatter slope of the runaway speed curve.
- the step between Kaplan and Francis curves is explained by noting that the runaway speed values for Kaplans are off-cam and thus correspond to the most unfavorable combination of wicket gates and runner blades position; this of course does not apply to Francis machines.

Fig. 6. Ratio between runaway and rated speed versus specific speed.

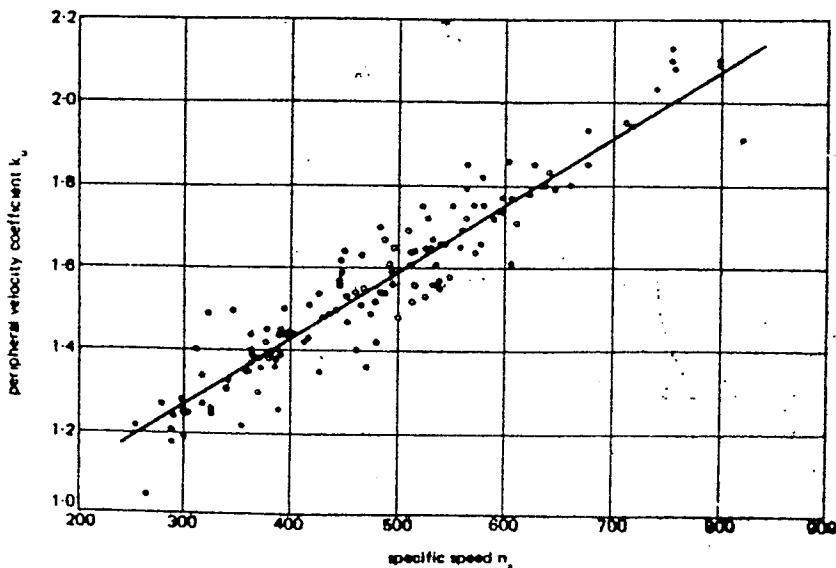
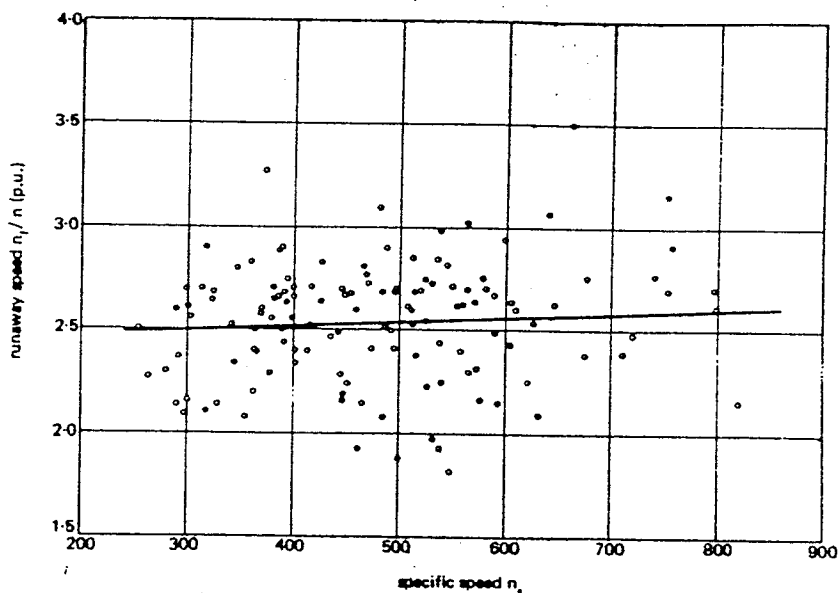
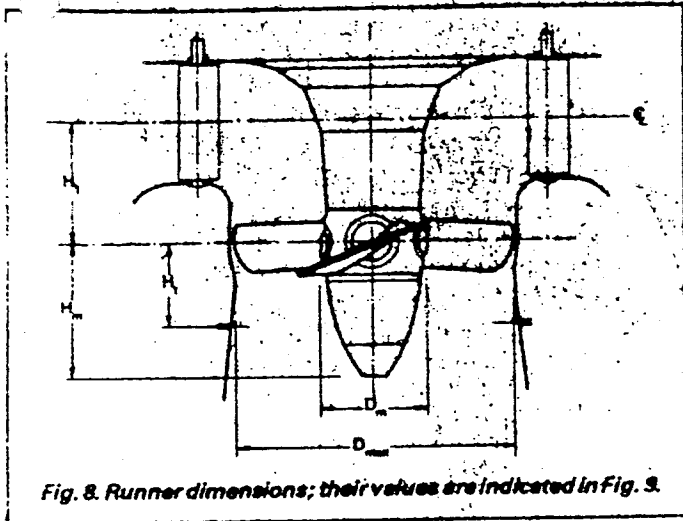


Fig. 7. Peripheral velocity coefficient versus specific speed.



k_u for Kaplan turbines is about 20 per cent higher than for Francis types.

The other runner dimensions D_m , H_m and H_1 indicated in Fig. 8, may be obtained as functions of n_s from the curves of Fig. 9.

The interpolating functions of the various curves are as follows:

$$D_m/D_M = 0.25 + 94.64/n_s$$

$$r = 0.82 \quad s = 0.04$$

$$H_m/D_m = 6.94 n_s^{-0.403}$$

$$r = -0.62 \quad s = 0.07$$

$$H_1/D_m = 0.38 + 5.17 \cdot 10^{-5} n_s$$

$$r = 0.23 \quad s = 0.03$$

Combining Eqs. (1), (2), (3) and (4) with the capacity equation:

$$P = \gamma Q H_n \eta_t$$

and assuming a conventional efficiency value of $\eta_t = 0.93$, it is possible to write Q as a function of D_M and H_n in the following way:

$$Q = D_M^2 F(H_n)$$

The function $F(H_n)$, within the n_s values considered, ranges between 7.3 and 7.8 with a variation of only 7 per cent.

It is therefore possible to draw the conclusion from these statistical diagrams that as a first approximation the water flow of Kaplan turbines depends only on the square of the runner diameter.

Runner size

To determine the runner main dimensions, the peripheral velocity coefficient k_u as defined by the expression:

$$k_u = \pi D_M n / (60 \sqrt{2g H_n}) \quad (3)$$

is adopted.

The function $k_u = k_u(n_s)$ calculated by correlating the available data is:

$$k_u = 0.79 + 1.61 \cdot 10^{-3} n_s \quad (4)$$

with

$$r = 0.95 \quad s = 0.1$$

The corresponding curve is indicated in Fig. 7.

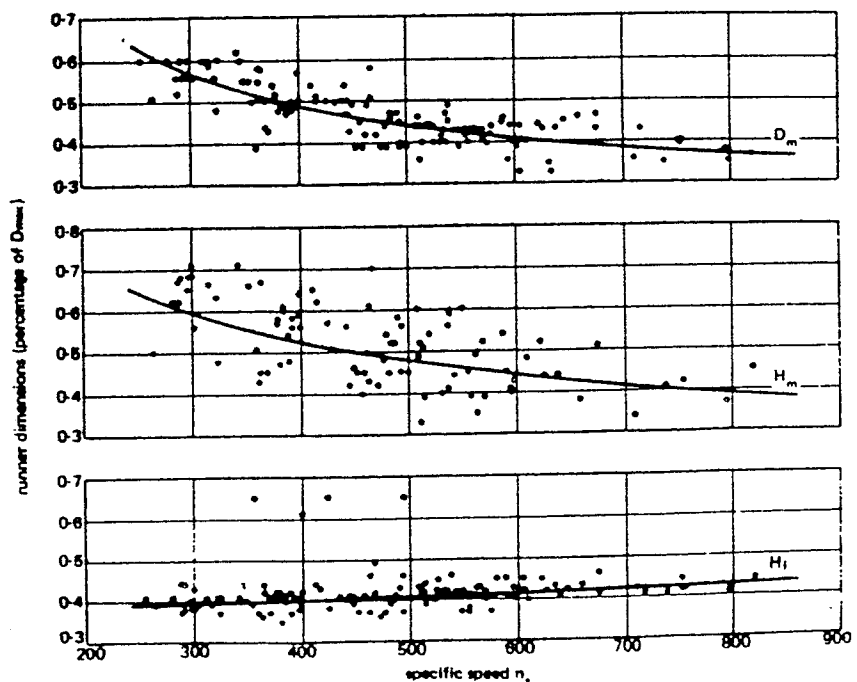
For a given value of n_s , the outer diameter of the runner can be then calculated using the formula

$$D_M = 84.5 k_u \sqrt{H_n} / n$$

It should be noted that for values of n_s around 300, the

(To be continued)

Fig. 9. Main runner dimensions versus specific speed.



Modern trends in selecting and designing Kaplan turbines

PART TWO

By F. de Siervo and F. de Leva*

Results of an extensive investigation carried out on more than 130 Kaplan turbines manufactured all over the world are presented in the form of statistical diagrams providing engineers with the latest information for preliminary design of hydro powerplants.

THE FIRST PART of this article presented a comprehensive table of Kaplan turbines used in major hydro schemes, and general trends in their manufacture and design were discussed and illustrated. It was suggested that the water flow of Kaplan turbines depends only on the square of the runner diameter.

Spiral case size

Both steel and concrete spiral cases have been investigated. The available data show that within the specific speed range between 400 and 600 approximately, both types may be adopted depending upon the particular characteristics of the powerplant. This n_s range corresponds roughly to a H_n range between 35 and 15 m. Steel spiral cases have been adopted for heads down to 15 m with rated capacity up to 70 MW, while concrete spiral cases are encountered for heads up to 40 m with capacities ranging between 50 and 100 MW.

The spiral cases for Kaplan turbines are usually designed using the same formulae as for Francis units:

$$Q\gamma = Q_0(1 - \sigma/2\pi)$$

$$v_w r_1 = k$$

that indicate the uniform feeding of the distributor along its circumference and the irrotationality of the water flow within the spiral case.

In the preceding formula the angle γ is measured in the direction of water flow starting from the spiral nose. Whereas for steel cases the enveloping angle is close to 60°, in concrete cases it is usually slightly above 180°, leading to smaller cross section dimensions.

The water flow for each turbine has been calculated from

the rated head and capacity values assuming a conventional efficiency of 93 per cent.

The velocity at the inlet section of spiral casings has been then obtained from the inlet dimensions as indicated in Fig. 10.

The available data are indicated in Fig. 11 together with the correlating curves which are, for steel spiral cases:

$$v_1 = 3.17 + 759.21/n_s$$

$$r = 0.26 \quad s = 1.04$$

Notations*

D_M	= Runner outer diameter (m)
g	= Gravity acceleration (m/s^2)
h_b	= Barometric pressure (m)
h_s	= Static suction head referred to the wicket gate centreline (m)
h_w	= Water vapour pressure (m)
H_n	= Turbine net design head (m)
k_n	= Runner peripheral velocity coefficient
k_{v1}	= Ratio between water velocity v_1 and spouting velocity
k_{v2}	= Ratio between water velocity v_2 and spouting velocity
n	= Turbine speed of rotation (rev/min)
n_f	= Turbine runaway speed of rotation (rev/min)
n_s	= Turbine specific speed
P_t	= Turbine design capacity (kW)
Q_0	= Turbine rated flow (m^3/s)
$Q\gamma$	= Flow passing through a spiral case radial section rotated by the angle γ in respect of the spiral nose (m^3/s)
r	= Statistical curves correlation coefficient
r_1	= Distance of a point in the spiral case from the turbine axis (m)
s	= Statistical curves standard deviation
v_1	= Water velocity at steel spiral cases inlet section (m/s)
v_2	= Water velocity at concrete cases inlet section (m/s)
v_3	= Water velocity at draft tube inlet section (m/s)
v_w	= Peripheral velocity of water in the spiral case
σ	= Cavitation coefficient (Thoma's coefficient)

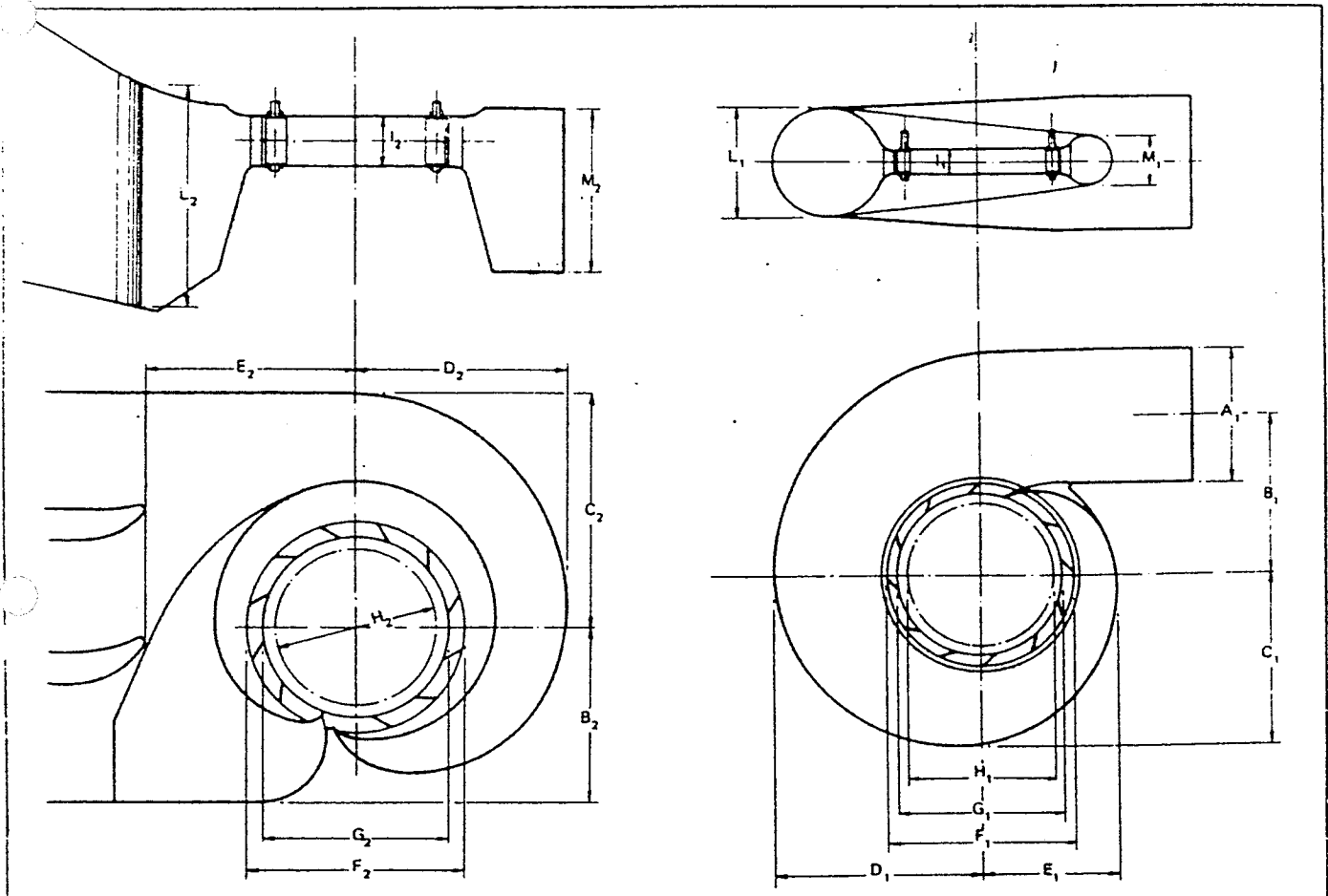


Fig. 10. Main concrete spiral case (left) and steel spiral cases dimensions (right). Their values are indicated in Figs. 12 and 13.

and for concrete spiral cases:

$$v_2 = 2.44 - 1.19 \cdot 10^{-3} n_s$$

$$r = -0.32 \quad s = 0.39$$

This shows that the water velocity for steel spiral cases is about 2.5 times greater than that in concrete spirals.

In addition it appears that in the case of Francis turbines water velocity is about 28 per cent higher than the velocity for Kaplan turbines with the same specific speed.

The marked scattering of the v_1 curve data may be a result of the inaccuracies in the evaluation of the inlet diameter A related to the presence of a conical inlet extension in several spiral cases.

The main dimensions of the spiral cases, as indicated in Fig. 10, are shown, as a function of n_s and referred to the diameter D_M , in Figs. 12 and 13.

The interpolating functions for the different curves are:

$$A_1/D_M = 0.40 n_s^{0.56}$$

$$r = 0.39 \quad s = 0.12$$

$$B_1/D_M = 1.26 + 3.79 \cdot 10^{-4} n_s \quad B_2/D_M = 1/(0.76 + 8.92 \cdot 10^{-4} n_s)$$

$$r = 0.25 \quad s = 0.12 \quad r = 0.71 \quad s = 0.21$$

$$C_1/D_M = 1.46 + 3.24 \cdot 10^{-4} n_s \quad C_2/D_M = 1/(0.55 + 1.48 \cdot 10^{-4} n_s)$$

$$r = 0.11 \quad s = 0.24 \quad r = 0.03 \quad s = 0.16$$

$$D_1/D_M = 1.59 + 5.74 \cdot 10^{-4} n_s \quad D_2/D_M = 1.58 - 9.05 \cdot 10^{-4} n_s$$

$$r = 0.22 \quad s = 0.20 \quad r = -0.06 \quad s = 0.14$$

$$E_1/D_M = 1.21 + 2.71 \cdot 10^{-4} n_s \quad E_2/D_M = 1.48 - 2.11 \cdot 10^{-4} n_s$$

$$r = 0.20 \quad s = 0.11 \quad r = -0.01 \quad s = 0.25$$

$$F_1/D_M = 1.45 + 72.17/n_s \quad F_2/D_M = 1.62 - 3.18 \cdot 10^{-4} n_s$$

$$r = 0.32 \quad s = 0.12 \quad r = -0.03 \quad s = 0.12$$

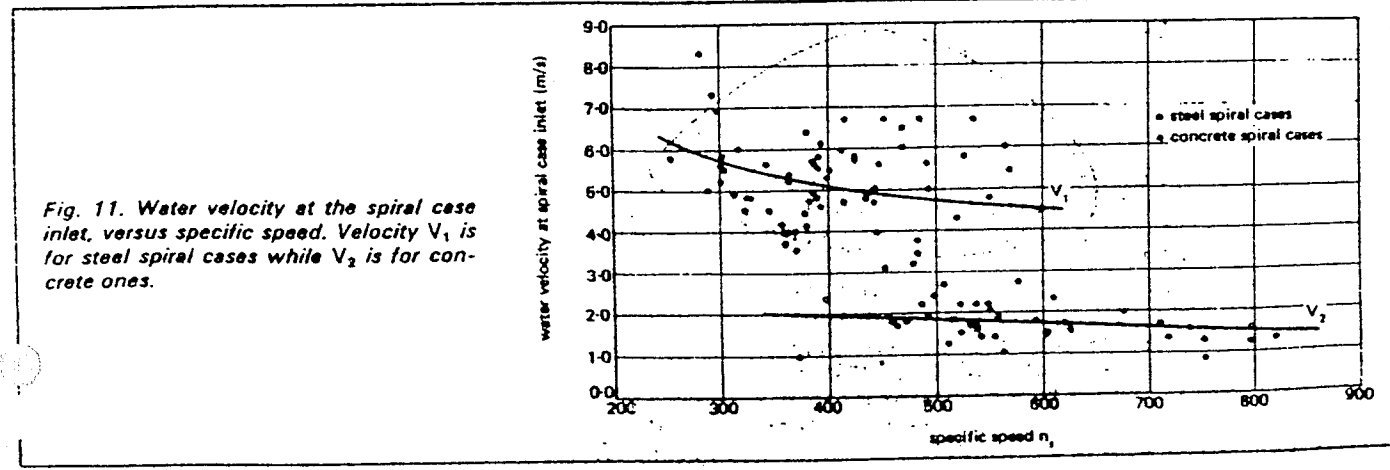


Fig. 11. Water velocity at the spiral case inlet, versus specific speed. Velocity V_1 is for steel spiral cases while V_2 is for concrete ones.

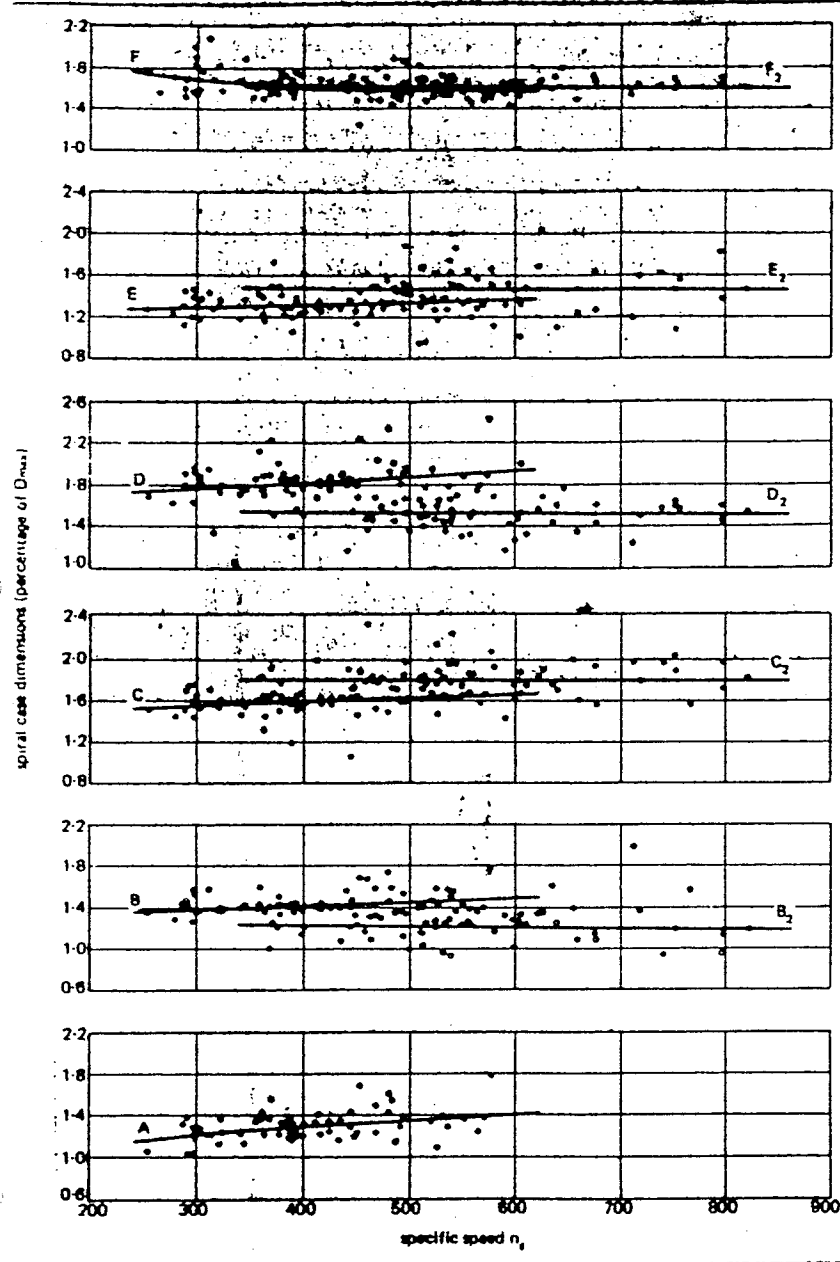


Fig. 12. Main spiral case dimensions versus specific speed. The letters refer to Fig. 10. Subscript 1 is for steel spiral cases while subscript 2 is for concrete ones.

$$\begin{aligned}
 G_1/D_M &= 1.29 + 41.63/n_s & G_2/D_M &= 1.36 + 7.79/n_s & r &= 0.28 & s &= 0.08 & r &= -0.04 & s &= 0.06 \\
 H_1/D_M &= 1.13 + 31.86/n_s & H_2/D_M &= 1.19 + 4.69/n_s & r &= 0.31 & s &= 0.05 & r &= 0.05 & s &= 0.03 \\
 I_1/D_M &= 0.45 - 31.80/n_s & I_2/D_M &= 0.44 - 21.47/n_s & r &= -0.48 & s &= 0.03 & r &= -0.23 & s &= 0.03 \\
 L_1/D_M &= 0.74 + 8.7 \cdot 10^{-4} n_s & L_2/D_M &= 1.44 + 105.29/n_s & r &= 0.58 & s &= 0.10 & r &= 0.15 & s &= 0.23 \\
 M_1/D_M &= 1/(2.06 - 1.20 \cdot 10^{-4} n_s) & M_2/D_M &= 1.03 + 136.28/n_s & r &= -0.404 & s &= 0.11 & r &= 0.21 & s &= 0.19
 \end{aligned}$$

The ratios Kv_1 and Kv_2 between the water velocity v_1 and v_2 at spiral case inlet and the spouting velocity corresponding to the rated head, obtained according to Fig. 1 and 11, are indicated in Fig. 14.

They increase with the increase of n_s although the velocities v_1 and v_2 diminish appreciably. The two opposing ends, which influence the design of Francis turbines, that to contain the head losses as percentages of the net head and to limit the dimensions of the spiral cases, play the same role both for concrete and for steel spiral cases of Kaplan turbines.

Figures 12 and 13 show that for a given n_s the concrete spiral case definitely permits smaller cross section dimensions than steel cases. For instance, considering the specific speed $n_s = 500$, the following cross-sectional widths are obtained:

- steel cases: width = $B_1 + C_1 + A_1/2 = 3.76 D_M$
- concrete cases: widths = $B_2 + C_2 = 3.04 D_M$

with a difference of about 24 per cent.

This is because of both the smaller enveloping angle of the concrete cases (already made evident) and the different shape of the volute cross section.

Some interesting observations can be made by comparing the dimensions of steel spiral cases for Francis and Kaplan turbines.

The curves relating to the dimensions A , L and M display a strong measure of agreement within the area of overlapping specific speeds. Increasing the n_s value the dimensions of Kaplan cases increase practically with a constant rate that roughly corresponds to the square root of the decreasing water velocity at the spiral case inlet; this confirms that the water flow does not depend appreciably on the n_s value, as suggested earlier.

The dimensions F_1 , G_1 and H_1 for Kaplan scrolls remain

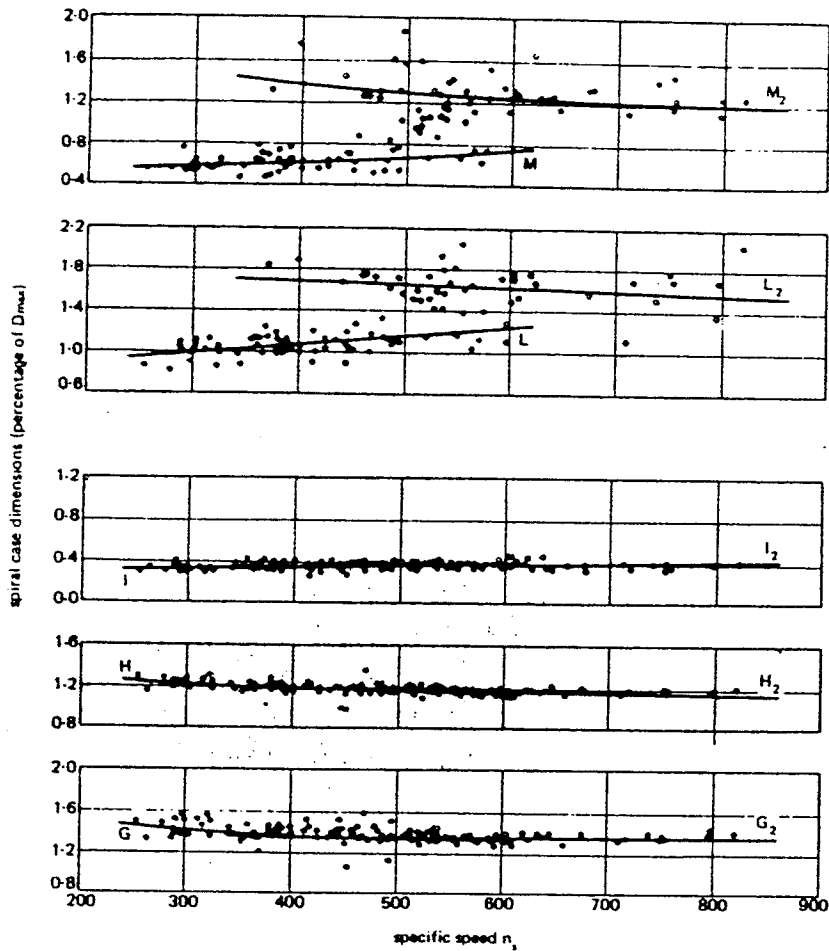


Fig. 13. Main spiral case dimensions versus specific speed. The letters refer to Fig. 10. Subscript 1 is for steel spiral cases. Subscript 2 is for concrete ones.

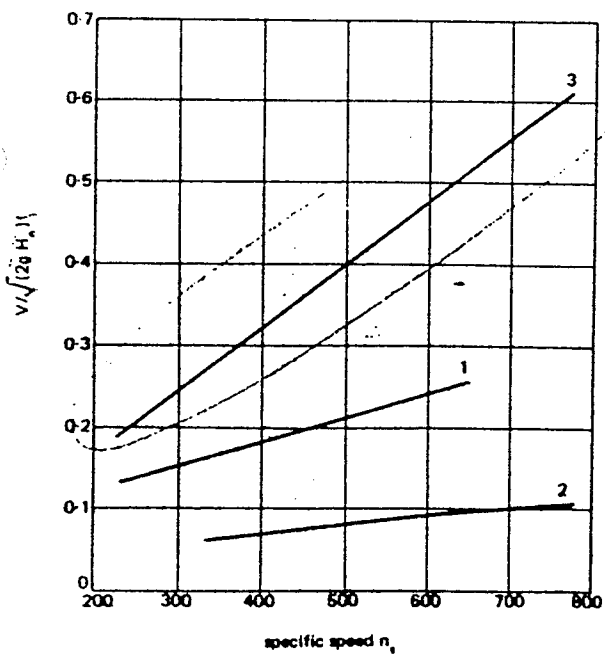


Fig. 14. Ratio between actual and spouting velocity in (1) steel spiral case inlet, (2) concrete spiral case inlet, (3) draft tube inlet.

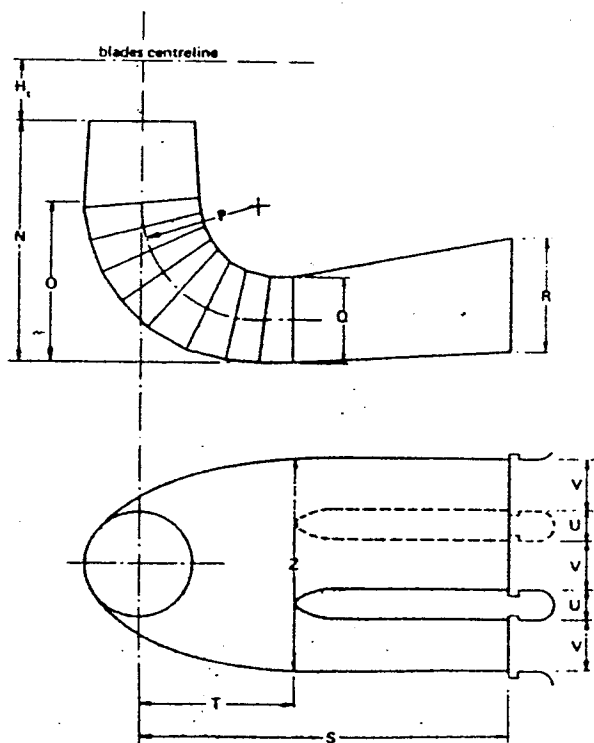
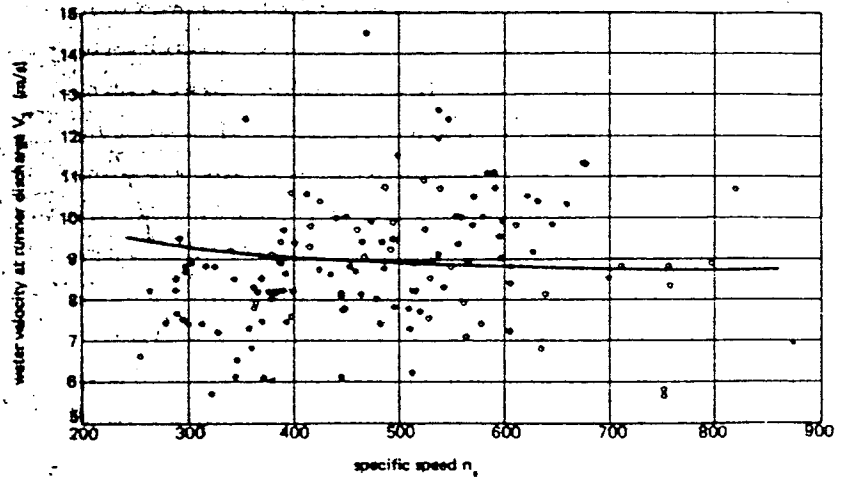


Fig. 15. Main draft tube dimensions. Their values are indicated in Fig. 17.

Fig. 16. Water velocity at draft tube inlet section versus specific speed n_s .



more or less constant with increasing n_s , while they diminish for Francis turbines. This is because the runner geometry of Francis turbines changes considerably with increasing n_s (the ratio between inlet and outlet diameter of Francis runners decreases) while this does not occur in Kaplan machines.

As a consequence the cross and longitudinal section dimensions B_1 , C_1 , D_1 and E_1 that decrease with increasing n_s for Francis turbines, show the opposite trend in the case of Kaplan machines.

For concrete spiral cases the dimensions B_2 , C_2 and L_2 appear to be constant, while water velocity v_3 decreases with increasing n_s . This does not conflict with the fact that the water flow depends mainly on the runner diameter alone, because for increasing n_s the scroll piers became thinner, thus allowing the net inlet area to increase in the same proportion that the water velocity decreases.

Draft tube size

The draft tube dimensions are directly related to the runner size and to the absolute velocity at its inlet section.

Fig. 16 gives the mean statistical value of this velocity versus the specific speed n_s . The interpolating function is:

$$v_3 = 8.42 + 250.25/n_s$$

where

$$r = 0.36 \quad s = 1.51$$

The most important dimensions of the draft tube indicated in Fig. 15 are given by Fig. 17; the interpolating functions are:

$$H_i/D_M = 0.24 + 7.82 \cdot 10^{-6} n_s$$

$$r = 0.06 \quad s = 0.15$$

$$N/D_M = 2.00 - 2.14 \cdot 10^{-4} n_s$$

$$r = 0.079 \quad s = 0.31$$

$$O/D_M = 1.40 - 1.67 \cdot 10^{-5} n_s$$

$$r = -0.10 \quad s = 0.23$$

$$P/D_M = 1.26 - 16.35/n_s$$

$$r = -0.06 \quad s = 0.15$$

$$Q/D_M = 0.66 - 18.40/n_s$$

$$r = -0.15 \quad s = 0.07$$

$$R/D_M = 1.25 - 7.98 \cdot 10^{-6} n_s$$

$$r = -0.07 \quad s = 0.15$$

$$S/D_M = 4.26 + 201.51/n_s$$

$$r = 0.18 \quad s = 0.63$$

$$T/D_M = 1.20 + 5.12 \cdot 10^{-4} n_s$$

$$r = 0.25 \quad s = 0.25$$

$$Z/D_M = 2.58 + 102.66/n_s$$

$$r = 0.16 \quad s = 0.4$$

The figures show that the dimensions of Kaplan draft tubes are closely matched to the corresponding dimensions of those of Francis turbines in the overlapping area.

For increasing n_s the dimensions do not vary appreciably, except that the draft tube length S decreases.

Fig. 14 indicates that the kinetic energy stored within the draft tube increases, as a percentage of the total available energy, with increasing n_s , reaching values much greater than those relevant to Francis turbines.

This makes it convenient from both technical and economical points of view, not to reduce the dimensions of the draft tube as is normal for Francis turbines, but rather to keep them constant as a function of n_s .

Comparison between Francis and Kaplan turbines

It is interesting to make a comparison between Francis and Kaplan turbines in the head range common to both machines.

For this purpose, having chosen a head of 50 m, two machines having the same capacity of 50 MW have been sized according to the statistical diagrams previously given.

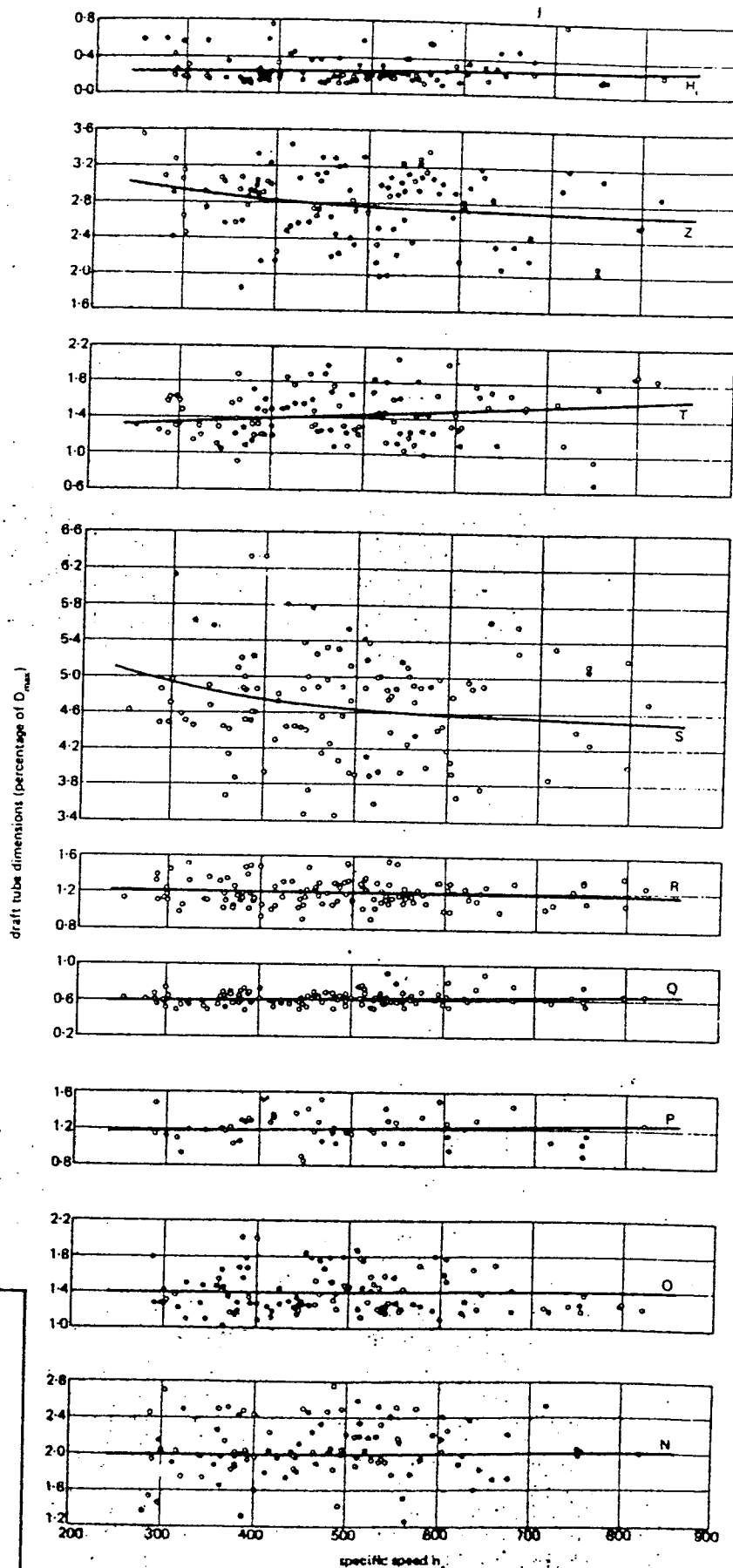
The main design data and dimensions of the two machines are given in Table II.

Fig. 18 shows sketches of both turbines where the centreline elevation is referred to the same tailrace water level.

Table II—Comparison of Francis (F) and Kaplan (K) turbines for the same head and rating

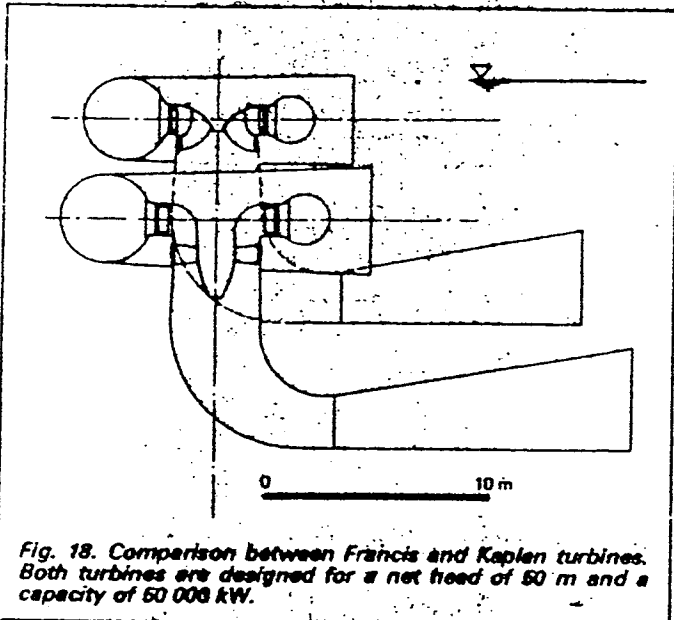
	F	K
H_n (m)	50	50
P (kW)	50 000	50 000
n_s	310	358
n (rev/min)	179	213
D_s (m)	3.55	
D_M (m)		3.83
D_m (m)		1.54
A (m)	4.03	4.95
$E + D$ (m)	10.11	11.80
H_t (m)		1.03
N (m)	7.88	7.66
S (m)	16.19	18.47
H_s (m)	-1.8	-6.3

Fig. 17. Main draft tube dimensions versus specific speed. The letters refer to Fig. 15.



CORRECTIONS

In the interpolating functions referred to on P56 in Part I of this article, D_m should read D_M .



the statistical curves of the machine operating characteristics that are well in accordance with those deduced from the physical dimensions. This is well exemplified by observations made about the dependence of the water flow on the runner diameter, as confirmed by the results of sizing criteria for the spiral cases.

This validates the correlation functions obtained and the uniformity of the design criteria adopted by the different manufacturers.

As for Francis turbines, the trend is evidently towards higher specific speeds and thus to smaller and more economical installations. □

Acknowledgements

The authors wish to thank all the manufacturers indicated in the annexed table for the valuable contribution in supplying the main design data and the dimensions of their machines, that made possible the present study.

References

1. DE SIERYO, F. AND DE LEVA, F. "Modern trends in selecting and designing Francis turbines", *Water Power and Dam Construction*, August 1976.
2. MAGNET, E. "Das Draukraftwerk Freistritz-Ludmannsdorf der Österr. Draukraftwerk AG", *Der Bauingenieur*, October 1968.
3. "The Kainji development", *Water Power*, September 1967.
4. WILLETT, D. C. "The Mactaquac development", *Water Power*, November 1966.
5. "Les équipements hydroélectriques du Rhin de Bâle à Strasbourg Electricité de France, Paris, France.
6. "Die 100 000-PS-VOITH-Kaplan turbinen der Donaukraftwerks ASCHACH", J. M. Voith GmbH, Heidenheim, Germany.
7. "100 000-PS-Kaplan turbinen im Kraftwerk Très Marias", J. M. Voith GmbH, Heidenheim, Germany.
8. "Samarra Hydroelectric Power Plant", GIE, Italy.
9. "Jupia Hydroelectric Power Plant", GIE, Italy.
10. GUIDETTI, G. AND SAVOYE, R. "Douze turbines Kaplan de construction récente", *Bulletin Technique Vevey*, 1970.
11. "Hitachi Kaplan turbine", Hitachi Limited, Tokyo, Japan.
12. "Turbines Hydrauliques", Energomachexport, Moscow, USSR, 1971.
13. KOVALEV, N. N. "Hydroturbines design and construction", Israel Program for Scientific Translations, Jerusalem, 1965.
14. COEN, M. "Macchine Idrauliche", Signorelli, Milano, 1974.
15. SHCHEGOLEV, G. "Problems in designing and constructing large turbines", *Water Power*, April 1974.
16. "The Drau river projects" (Feistritz), *Water Power* February 1969.

Even taking into proper account the fact that the turbines were sized according to statistical data and not on the basis of actual model test results, the advantage of Francis turbines is evident on the basis of purely economical considerations.

Special powerplant requirements particularly broad head ranges, and the necessity to have smooth operation with high efficiency even at very reduced capacities, sometimes dominate economic considerations as is shown by the appreciable number of Kaplan turbines installed with heads between 40 and 60 m.

Conclusions

The present investigation shows the limited scattering of data for most of the curves drawn, particularly those relevant to the peripheral velocity coefficients and the runner dimensions.

Furthermore the number of powerplants studied has made it possible to draw theoretical deductions based on